Eur. Phys. J. Plus (2024) 139:475
https://doi.org/10.1140/epjp/s13360-024-05222-y

THE EUROPEAN PHYSICAL JOURNAL PLUS

Regular Article

Mapping the elemental distribution in archaeological findings through advanced Neutron Resonance Transmission Imaging

Giulia Marcucci[1,2,a], **Antonella Scherillo**[2], **Maria Pia Riccardi**[3], **Costanza Cucini**[4], **Quentin Lemasson**[5], **Daniela Di Martino**[1]

[1] Dipartimento di Fisica "G. Occhialini", Università degli Studi di Milano-Bicocca and INFN Sezione di Milano-Bicocca, Piazza della Scienza 3, 20126 Milan, Italy
[2] ISIS Neutron and Muon Source, Chilton-Didcot OX11 0QX, UK
[3] Dipartimento di Scienze della Terra e dell'Ambiente and Arvedi Laboratorio– sede di Pavia, Università degli Studi di Pavia, via Ferrata 9, 27100 Pavia, Italy
[4] IRAMAT, UMR 7065, CNRS, Université de Technologie Belfort Montbéliard, 90010 Belfort Cedex, France
[5] Ministère de la Culture/Chimie ParisTech, 14 Quai François Mitterrand, 75001 Paris, France

Received: 23 December 2023 / Accepted: 28 April 2024

Abstract This work highlights recent application of energy-selective neutron imaging at the ISIS Neutron and Muon Source, specifically focusing on the development of Neutron Resonance Transmission Imaging (NRTI) at the INES instrument. NRTI is a nuclear technique based on resonant neutron absorption reaction, which combines the sensitivity to elemental and isotopic composition with detailed morphological information, using the epithermal portion of the neutron flux available on the INES instrument at the ISIS facility. Unlike standard neutron radiography and tomography methods, NRTI preserves detailed time and energy information for each detector pixel, enabling enhanced visualisation of elemental distribution inside an object's volume, with the potential for quantitative elemental analysis. These features combined with the non-destructiveness of NRTI make the method promising for applications in the field of Cultural Heritage, especially when it is employed in a multi-technique approach to provide complementary information about the composition and the crystalline structure of archaeological artefacts. A study related to Heritage Science is presented to demonstrate the effectiveness of NRTI in non-destructive investigations of inhomogeneous artefacts, specifically focusing on the excavation finds related to the first evidence of ancient brass production in Milan, Italy, during Roman times.

1 Introduction

In recent years, neutron imaging established its strengths and extraordinary versatility for non-destructive investigation of many kinds of morphological and microstructural properties of materials [1–9], as proved by the increase in its availability at neutron sources worldwide, providing fully complementary information concerning conventional imaging techniques based on other probes such as X-rays [10–16]. The rapid development of neutron imaging methods and detection systems has led to a striking improvement in resolution and efficiency, as well as in techniques based on a broad range of contrast mechanisms, making imaging with neutron beams indispensable in modern research.

As a result of their intrinsic properties, neutrons interact with matter differently with respect to electrons, protons or X-rays: due to their neutral charge, they interact when in short-range proximity ($\sim 10^{-15}$ m) with the nucleus of an atom, resulting in a highly penetrating capability of the order of centimetres, depending on the material. This feature has three important consequences: (i) neutrons can be used to investigate microscopic properties of dense matter non-destructively; (ii) they can be used as a bulk probe of matter, overcoming issues related to surface effects/structures, and (iii) and to investigate objects in complex sample environments.

Moreover, neutrons are an optimum probe for observing light atoms, such as hydrogen, as well as for distinguishing neighbour elements in the periodic table. In addition, they are the only scattering probes able to provide isotopic contrast.

The current state of the art of neutron imaging techniques is highly advanced. This work, in particular, aims to provide details into the recent advancement of the 4D Neutron Resonance Transmission Imaging (NRTI) technique [17–19] developed at the INES beamline of the ISIS spallation neutron source [20–22]. Conventionally, neutron imaging often uses cold or thermal neutron beams. However, another rather promising energy range not yet widely used for imaging purposes is the epithermal range, which is exploited for the NRTI technique. High epithermal neutron fluxes are available at neutron spallation sources, enabling the isotopic and elemental characterisation of materials thanks to the presence of intense peak structures (called resonances) in the neutron-induced

[a] e-mail: giulia.marcucci@unimib.it (corresponding author)

Published online: 03 June 2024

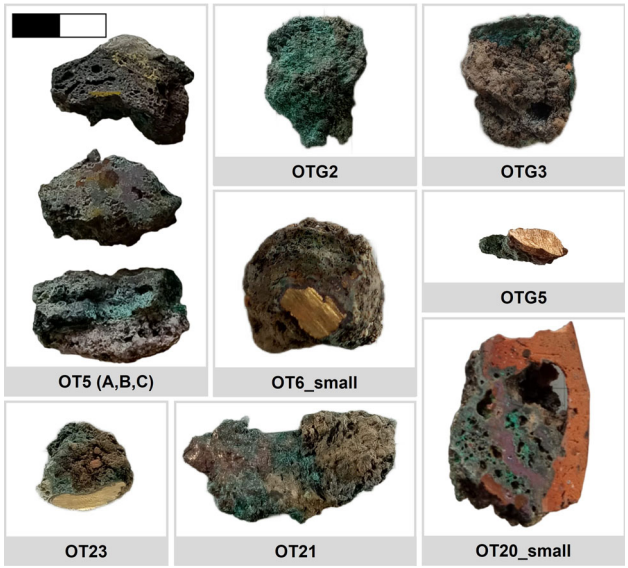

Fig. 1 Pictures of the crucible fragments analysed through neutron resonance absorption spectroscopy techniques. Metallic depositions are evident on the surface of some of these fragments, and the alloy colour suggests a composition related to brass

reaction cross sections. The NRTI technique is based on the resonant absorption of the incident epithermal neutrons, resulting in a transmitted neutron beam containing characteristic dips univocally related to the material's elemental and isotopic composition.

What sets NRTI apart from standard neutron radiography/tomography is the possibility to conduct simultaneously three-dimensional (3D) mapping with spectroscopic information (4D) and potentially quantitative imaging. In fact, for phenomena based on resonant neutron capture, the absorption of neutrons is the dominant interaction and the relative cross section can be exactly calculated; therefore, quantitative analysis is possible. Moreover, NRTI enables the enhancement of the contrast of specific elements compared to others (in particular those with similar neutron attenuation coefficients for standard tomography) inside the bulk of an object, thanks to the full energy spectrum acquired in each detector pixel. Furthermore, this technique is one of the first imaging methods that can be used for isotopic imaging.

In this work, a study related to Cultural Heritage is presented to describe the unique features of NRTI for investigating with enhanced contrast and isotopic sensitivity the elemental composition and distribution inside archaeological objects, especially those with inhomogeneous structures. These characteristics, combined with the non-destructive nature of the method, make NRTI a promising and powerful imaging tool for applications in the field of Heritage Science, expanding the potential of neutron imaging and providing complementary information to other more conventional techniques for non-destructive characterisation of an archaeological object.

2 Archaeological framework

In 2009, the excavation in Corso of Porta Romana 20, Milan (Italy), conducted by *Soprintendenza Archeologia, Belle Arti e Paesaggio di Milano*, unearthed numerous fragments of metals slug and crucibles related to brass production and datable between the end of I and the beginning of II century CE [23]. These excavation finds are the first evidence of at least one brass workshop activity in the ancient Roman city of Mediolanum [23, 24]. In fact, brass production was widespread throughout the Roman Empire [25] and well documented in England, Germany and France [26–28], but it was completely unknown in Italy.

These crucibles consist of mass-produced terracotta pots, coated with a thick layer of refractory clay. Inside, traces of copper and zinc heating can be found, as they were brought to high temperatures to liquefy the alloy and to throw it into moulds to produce brass appliques for furniture and ornamental objects.

A subset of the unearthed crucible fragments clearly shows metallic deposition on their surfaces while in others brass or, more generally, metallic inclusions can be inside their bulk.

Therefore, to disclose evidence of brass casting and confirm the composition of the metallic traces in a non-destructive way, from a set of about twenty crucible fragments, eight of them have been selected based on their size (a few centimetres of thickness), weight (as a rough indication of the presence of metallic inclusions in the volume) and superficial morphological properties to request access for elemental analysis through neutron resonance absorption spectroscopy (described in Sect. 3) at the INES beamline of the ISIS Neutron and Muon Source (UK). Considering the thickness of some centimetres, these samples may be opaque to conventional elemental techniques (such as X-ray fluorescence or Particle-Induced X-ray Emission); therefore, neutron techniques have been chosen as the method of analysis to access the composition deeper in the sample volumes. Figure 1 displays the pictures of the crucible fragments selected for non-destructive investigation.

3 Methods

NRTI is a spectroscopic method that relies on the interaction of neutrons via resonant absorption with the nuclei present in the sample. The analytical approach is based on the presence of intense peaks, known as resonances, in the neutron-induced reaction cross sections corresponding to an increased probability of absorption at specific neutron energies by several orders of magnitudes. The energy position of resonances differs for each nuclide, allowing for simultaneous elemental and isotopic identification for compositional analysis [29].

Two analytical techniques based on this type of interaction, NRCA and NRTI, have been exploited to investigate non-destructively the elemental composition and distribution of the Roman crucible finds, providing bulk information.

Both methods are based on Time-Of-Flight (TOF) measurements with epithermal neutrons (0.5 eV–10 keV), exploiting the pulsed nature of the ISIS Neutron and Muon Source.

NRCA, as well as NRTI, relies on well-established methodologies. NRCA is an optimised technique both conceptually and experimentally at ISIS to obtain qualitative and semi-quantitative compositional information. A summary of the main information and references about this method is provided in Sect. 3.1. Instead, more details will be provided for the NRTI method, as this paper aims to present recent advances in this technique at the ISIS facility, for its application in the field of Cultural Heritage. The qualitative elemental composition obtained through both NRTI and NRCA has been compared with Particle-Induced X-ray Emission (PIXE) analysis, which is a more established non-destructive method for quantifying the composition of archaeological objects made of a wide range of matrixes [30, 31]. PIXE investigations have been conducted at the Grand Louvre Accelerator for Elemental Analysis (NewAGLAE-ANR-10-EQPX-22)—Centre de recherche et de restauration des musées de France (C2RMF)—exploiting a 3-MeV proton beam 50 μm wide and five SSD-EDX detectors for the PIXE mode. Details about the experimental conditions and the procedure followed for PIXE data analysis are described in [32]. The measurements of certified reference materials representing copper and copper alloys, such as BS938, NIST1107, CTIF-4, CTIF-5 and CTIF-6, were carried out for calibration purposes at the beginning and the end of each experimental session following the same protocol adopted for the archaeological samples. Errors can be estimated as in [33], with values ranging from 1 to 10%, depending on the concentrations.

3.1 Neutron resonance capture analysis

The NRCA technique relies on the Time-Of-Flight (TOF) measurement of the prompt γ-rays emitted after neutron captures reactions in the material under investigation [29, 34]. The arrival time of the γ cascade following the neutron capture reaction is recorded on the detector instead of performing full energy spectroscopy. Thus, the Time of Flight (and therefore the energy) of the neutron captured by the sample is determined. The resulting TOF spectrum is characterised by (n,γ) resonance absorption peaks, whose positions in time or energy are obtained for determining qualitative information about the sample elemental composition, as detailed in Sect. 3.2.

At the ISIS spallation source, NRCA experiments are routinely performed at the INES beamline with a detection set-up consisting of 3 yttrium aluminium perovskite (YAP) scintillator crystals coupled to silicon photomultipliers positioned above the sample stage at about 1 m distance from the sample position [21]. The resonant capture experimental set-up is optimised for providing a qualitative and semi-quantitative evaluation of the elemental composition of an object. NRCA is particularly useful for detecting impurities whose capture cross sections are very intense at low energies. It can detect elements with resonances between 1 and 10 eV even at concentrations as low as tens of parts per million (ppm) [35] (for example, Au [21], Ag, Sb and As, which are of interest to Heritage Science).

3.2 Neutron resonance transmission imaging

The NRTI technique is an innovative extension of the Neutron Resonance Transmission Analysis (NRTA) [29, 34, 36] for conducting simultaneous spectroscopic and imaging analysis using a time- and space-resolved neutron detector. This method exploits the epithermal portion of a white neutron beam typically provided by a spallation source. For epithermal energies, resonance structures occur at distinct and at specific energies in the nuclide interaction cross sections with neutrons. Therefore, resonances can be used to identify and quantify the elemental, but also isotopic, composition of an object.

Spectroscopic information is collected through the TOF method, commonly used in a spallation source, and which relies on the measurements of the neutron arrival time on the detector relative to a trigger synchronised to the time of spallation (i.e. when the proton beam hits the target, the neutrons are produced by a spallation reaction). In this way, the neutron Time of Flights t can be converted into energies, in a non-relativistic regime:

$$E_n = \frac{mL^2}{2t^2}$$

where m is the neutron mass and L is the moderator to detector distance. L is calibrated using the main resonances of Gd and Ta foil samples, giving 23.44 m for this specific experimental campaign.

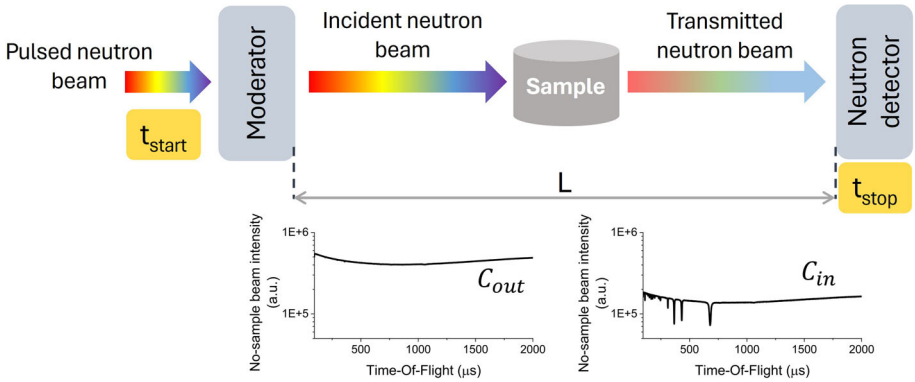

Fig. 2 Schematic representation of the NRTI technique based on TOF measurements. Spectroscopy measurements are possible by tracing back the neutron velocity (and therefore energy) using the known neutron flight path L and its time of flight, calculated as the difference between the stop signal measured by the detector and the start signal synchronised with the proton pulse delivered by the source. An example of a neutron spectrum incident on the sample (C_{out}) and transmitted through (C_{in}) is reported in time coordinates. An example of negative peaks related to resonant neutron absorption can also be seen in the transmitted spectrum

A schematic layout of the NRTI experimental set-up is represented in Fig. 2. In this case, the sample needs to be positioned as close as possible to the detector in order to reduce background noise due to scattering events and blurring due to the beam divergence. Since NRCA and NRTI require different sample-to-detector positions, separate runs of measurements have been acquired. The typical structure of the transmitted neutron beam presents negative dips whose positions in time/energy correspond to the absorption resonances responsible for neutron removal from the incident beam. The position of these dips allows for elemental and isotopic identification through comparison with the total cross sections of elements available in a nuclear database. In this case, a web-based radionuclide database program named KAERI was used [37].

In each detector pixel, the transmitted neutron beam as a function of the neutron TOF is recorded, which is directly related to the theoretical transmission T representing the fraction of the neutron beam traversing the sample without any interaction. Experimentally, the transmission T can be derived by alternating measurements of the transmitted neutron beam with (C_{in}) and without the sample (C_{out}), with background correction for both detected spectra (B_{in} and B_{out}) and normalisation to the ratio M between the neutron irradiation currents on the sample and detector (in the absence of sample):

$$T = M \frac{C_{\text{in}} - B_{\text{in}}}{C_{\text{out}} - B_{\text{out}}}$$

NRTI measurements have been conducted at the INES beamline of the ISIS Neutron and Muon Source (UK), which is one of the beamlines providing a high epithermal component in the white neutron flux, placing a commercial neutron Gas Electron Multiplier (nGEM) [38, 39] in the beamline.

The active area of the detector is 10×10 cm^2, and its pixel size is 0.8×0.8 mm^2. However, the effective area of investigation is limited to the maximum opening size of the jaws (beam 'delimiters' made of neutron absorbing materials) present on INES, which is 4.0×4.0 cm^2.

This detector is able to operate up to a total count rate of 10 MHz on the whole detector area. Moreover, each neutron is time stamped with a precision of 8 ns referred to the Tzero of the ISIS accelerator (i.e. the signal is synchronous to when the proton beam hits the target). Considering the time broadening of $\sim$400 ns affecting the initial neutron pulse due to the neutrons slowing down in the small water moderator [40, 41], the time binning of the NRTI acquisition has been set at 1 μs.

Considering the INES neutron flux reported in [42], the NRTI measurements of the crucible fragments lasted 2 days; each sample was irradiated for approximately 7 h, alternating acquisitions with and without the sample for normalisation purposes.

4 Results and discussion

At INES, NRCA is a routinely available technique, whereas NRTI is under development. Therefore, preliminary bulk elemental analysis was performed with NRCA to compare the NRTI results as both methods are based on TOF measurements of epithermal neutron absorption.

The NRCA spectra of the crucible fragments are shown in Fig. 3. The elements detected suggested the presence of bronze and brass alloys in the crucible fragments, with different amounts of secondary components like arsenic. The available TOF window of INES for useful NRCA signals is between 25 and 2000 μs. Below 25 μs, the background events (e.g. γ-flash coming from the source) are predominant over any useful signal peaks. Resonance capture peaks related to the presence of Cu and Zn are visible in the low TOF region (25–180 μs, see Table 1 for detailed positions and identification). Presence of Sn has been derived from the capture peaks at 38.8 and 109 eV and therefore occurring at 265 and 157 μs, respectively (Fig. 3).

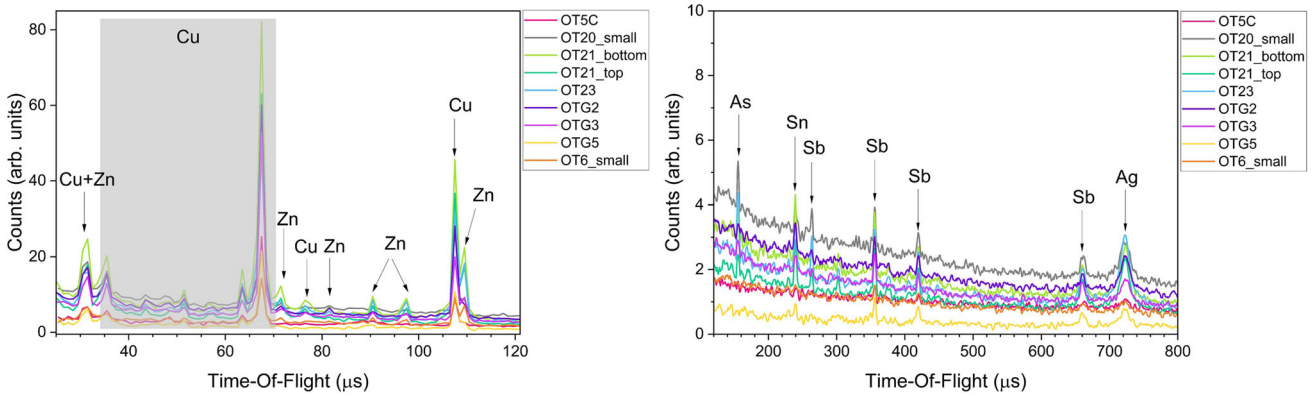

Fig. 3 NRCA spectra of the crucible fragments in the TOF region 25–120 μs and 120–1000 μs. The region between 1000 and 2000 μs has not been reported as it does not exhibit a significant signal for elemental composition determination. Main peaks related to copper, zinc, tin, arsenic, antimony, and silver are highlighted. Peaks within the grey box are related to copper. The qualitative composition of these fragments has been identified by comparing the resonance positions with capture (n ,γ) cross-section libraries [37]

Table 1 Neutron resonance capture peaks of copper and zinc identified in the low TOF region (25–180 μs, visible in Fig. 3) with 1 μs of uncertainty and the relative positions converted in energy

Element	Resonant capture peak	
	TOF (μs)	Energy (eV)
Cu	32.3	2610
Zn	32.3	2610
Cu	34.6	2050
Cu	44.7	1360
Cu	52.3	994
Cu	58.1	806
Cu	64.6	651
Cu	68.6	578
Zn	78.0	447
Cu	82.2	402
Zn	91.7	323
Zn	98.0	280
Cu	108.7	230
Zn	110.4	223

At higher TOF (>200 μs), the capture peaks of arsenic (46.9 eV/241 μs) and silver (5.17 eV/725 μs) have been identified as well as several peaks related to the presence of antimony in the 200–700-μs region (660 μs/6.3 eV, 420 μs/15.4 eV, 356 μs/21.4 eV and 302 μs/29.8 eV). The qualitative composition derived through NRCA is averaged on the entire volume of the samples, except for sample OT21, which is larger than the INES beam transverse size (4.0×4.0 cm^2). In this case, two separate measurements have been acquired (labelled as 'top' and 'bottom' in Fig. 3). Results are then averaged based on the effective irradiated volume, where both transverse sections measure 2.0×2.0 cm^2.

The same elemental composition of the fragments has been disclosed by NRTI measurements, as shown in Fig. 4. Both techniques are transparent to the refractory material matrix, which ensures that the detection of metallic elements is not affected by any background signal that may be generated by the crucible matrix.

Moreover, in the case of NRTI, neutron Time of Flights lower than 20 μs are accessible without background interference.

The element distribution inside the volume of the crucible fragments can be mapped through NRTI by selecting the resonance of a specific nuclide in the transmitted spectrum. As an example, the distribution of Cu, Zn, Sn, Sb and Ag inside the bulk of sample 'OT20_small' is shown in this work. In particular, this crucible fragment does not have any extended metallic deposition visible on its surface (only a few microscopic droplets) and has a homogeneous thickness. Figure 5 shows the neutron radiography of fragment 'OT20_small' obtained through NRTI. Different levels of transmission can be seen due to a different composition inside the bulk.

By selecting the TOF/energy range of a specific resonance dip in the relative NRTI spectrum (Fig. 4), such as the Cu resonance around 2 keV, the contrast due to the absorption of neutrons by copper nuclei is enhanced in the 2D map, revealing the position of only copper inside the volume (Fig. 6). The same procedure can be made with resonances related to the other elements (Fig. 6), to facilitate the visualisation of the elemental distribution even for nuclide with similar neutron attenuation coefficient. Regarding the

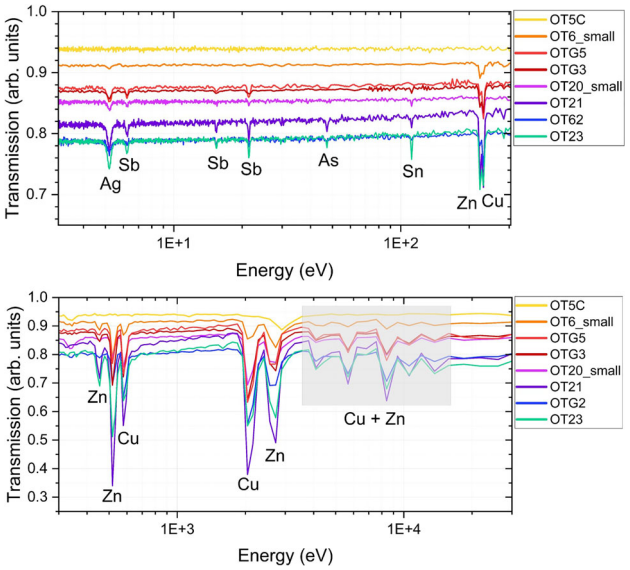

Fig. 4 NRTI spectra of the whole volume of the 8 crucible fragments shown in Fig. 1. Main peaks related to copper, zinc, tin, arsenic, antimony and silver are highlighted. Peaks within the grey box are related to a superposition of copper and zinc resonances. The qualitative composition of these fragments has been identified by indexing the resonance positions and comparing them with (n, tot) cross-section libraries [37]

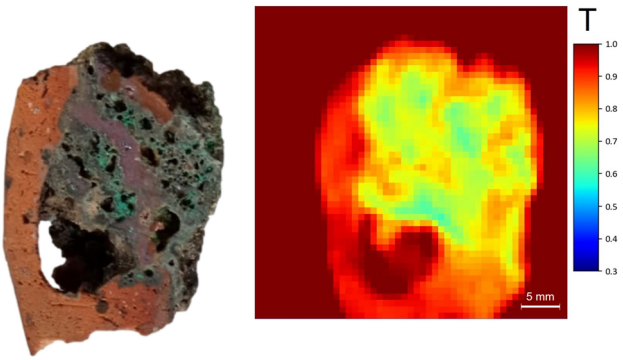

Fig. 5 Picture and transmission map of crucible fragment 'OT20_small'. The size of the 2D map is 4.0×4.0 cm^2

sample 'OT20_small', the following resonances have been selected, taking special account in selecting only those structures that do not overlap with other peaks of the other elements present in the bulk: 5.20 eV (Ag), 6.20 eV (Sb), 112 eV (Sn) and 515 eV (Zn). An example of the off-resonance selection is also provided to show that, with the selection of a region in the transmission spectrum without resonant absorbing dips, it is no longer possible to distinguish the distribution of different elements, but only thickness and overall absorption effects are predominant.

A preliminary quantitative estimation of the Zn and Sn content in sample OT20_small can be made to assess the nature of the copper alloy present inside the fragment under consideration.

Considering the known relationship between the experimental transmission and the concentration of an element as reported in the literature [34], the concentration of detected elements in the whole volume has been estimated as follows: zinc 26%, tin 6%, antimony 1.6% and silver 0.3%; considering the presence of any other trace elements would not significantly alter the concentration of major elements such as zinc and tin. The uncertainties can be estimated at 15% since the integration routine is not fully optimised and the NRTI calibration is still in progress, with simulations to account for effects related to strong absorbing materials and thickness. A forthcoming publication detailing the calibration of the technique is currently underway.

The qualitative composition obtained through NRCA/NRTI and the quantification derived through NRTI have been compared with PIXE analysis, initially employed prior to neutron analysis to check the crucibles composition with a full optimised method for elemental composition analysis. PIXE is a non-destructive method more consolidated for the quantification of major, minor and trace elements in a wide range of sample matrixes. However, superficial metallic depositions that can be investigated with PIXE are present only on 4 crucible fragments (metallic layers on samples OTG5, OT23 and OT6_small and a few droplets on sample OT20_small). Table 2 contains the quantitative composition of several metallic spots, highlighting the complementarity between bulky neutron investigations and PIXE, which is limited to tens of micrometres in thickness [43]. In particular, in sample 'OT20_small', different droplets of metal can be traced back to copper and its contaminants, from which it is not possible to deduce brass or bronze production. NRCA and NRTI complete the picture of the composition: thanks to the fact that the entire fragments volume can be analysed and to the high interaction cross sections with certain elements, it was possible to recognise the presence of Zn and Sn even in small concentrations.

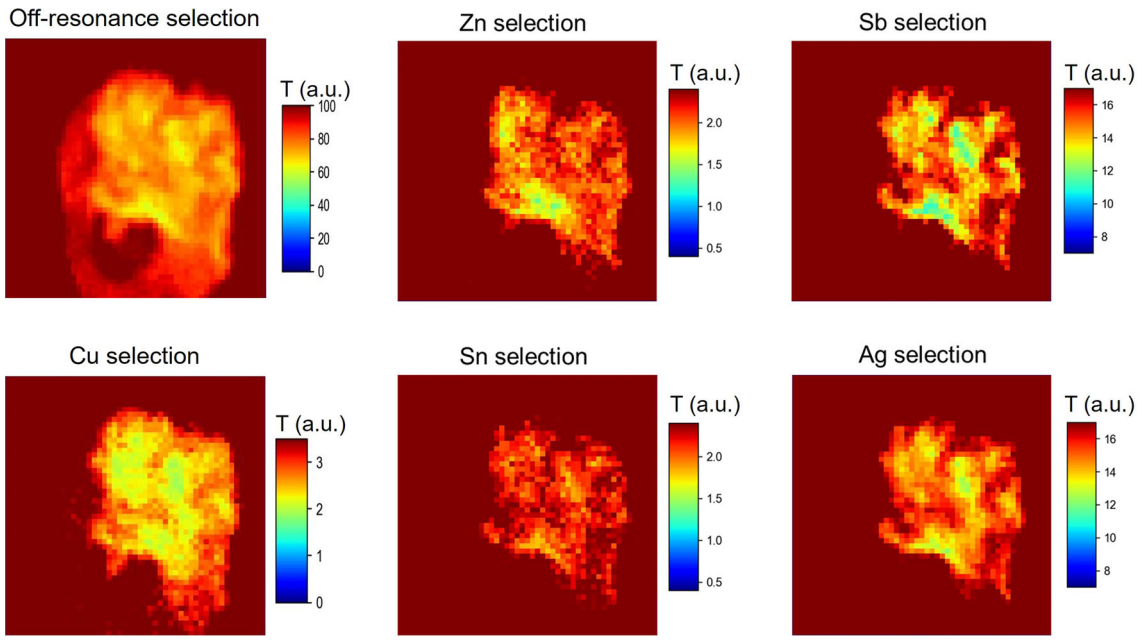

Fig. 6 NRTI maps after the selection of the main Zn, Sb, Sn, Cu and Ag resonances and of a TOF region without any absorption resonances. The size of all the 2D maps is 4.0×4.0 cm^2

Table 2 PIXE composition (in ppm) of metallic depositions (droplets and more extended layers) of the crucible fragments 'OT20_small', 'OTG5', OT6_small' and 'OT23'

Sample	Description	Fe	Ni	Cu	Zn	Ga	As	Ag	Sn	Sb	Pb #Lα
OT20_small	Metallic 'drop' #1	845	*u.d*	990,600	*u.d*	*u.d*	*u.d*	*u.d*	0	0	3300
OT20_small	Metallic 'drop' #2	846	586	990,200	0	0	*u.d*	*u.d*	*u.d*	*u.d*	3600
OT20_small	Metallic 'drop' #3	319	*u.d*	996,800	*u.d*	0	*u.d*	*u.d*	0	*u.d*	2430
OT20_small	Metallic 'drop' #4	332	*u.d*	994,200	*u.d*	*u.d*	*u.d*	*u.d*	0	*u.d*	2500
OTG5	Metallic 'drop' #1	1730	907	901,800	71,980	0	886	*u.d*	*u.d*	*u.d*	17,690
OTG5	Metallic 'drop' #2	1720	*u.d*	899,600	70,640	*u.d*	*u.d*	*u.d*	*u.d*	*u.d*	19,530
OTG5	Metallic layer	1610	609	902,700	69,640	0	894	532	2440	2760	17,700
OTG5	Metallic layer	1740	506	900,500	69,730	*u.d*	656	564	2200	2300	21,690
OTG5	Metallic layer	1690	491	886,000	67,370	0	1440	481	2170	2530	36,860
OT6_small	Metallic 'drop'	2800	762	751,500	214,600	826	*u.d*	*u.d*	3440	0	22,130
OT6 small	Metallic layer	2890	834	750,100	214,200	0	*u.d*	*u.d*	3630	*u.d*	24,740
OT6 small	Metallic layer	2930	801	744,600	211,900	440	0	368	3980	1140	32,990
OT6 small	Metallic layer	2960	825	752,700	214,600	425	*u.d*	*u.d*	3840	1350	21,640
OT6 small	Metallic layer	1750	912	743,500	165,100	*u.d*	938	510	31,980	2300	56,870
OT23	Metallic layer	1800	844	734,400	162,500	0	1090	*u.d*	32,090	*u.d*	67,640
OT23	Metallic layer	1820	799	764,000	171,200	552	435	553	32,370	1640	30,400

Other elements not included in the table were not disclosed with PIXE (such as Mn, Co, In, Au, etc.). u.d. means below the detection limit. Errors can be estimated as in [33], with values ranging from 1 to 10%, depending on the concentrations

The quantification attempt using NRTI revealed a zinc and tin content that can be traced back to brass production. In addition, imaging performed through NRTI confirms the presence of brass in several areas, not visible by naked eye, more extensively than with small superficial analyses.

In this way, it is possible to confirm the presence of a workshop dedicated to the processing of brass in the ancient city of Mediolanum, since it is known from the literature that in Roman brass both tin and zinc are often present in the alloy [44].

Moreover, the detection through NRTI and NRCA of very small amounts of arsenic can be useful to characterise the alloy [45], as well as of Sb and Ag which may be present as contaminants of copper or other elements.

5 Conclusions

In the field of Heritage Science, neutron resonance absorption spectroscopy is a powerful method for determining non-destructively the elemental composition of thick samples thanks to the high penetrating capability of neutrons and the presence of resonance peaks in the neutron-induced absorption cross sections of nuclei. The application of these techniques can be now necessary for non-destructive investigations of thick samples for which established probes such as X-rays cannot succeed. Neutron Resonance Capture Analysis is a well-optimised elemental analysis and is routinely applied at the INES beamline of the ISIS Neutron and Muon Source, but any capture peaks below 25 μs are overshadowed by the background. On the other hand, Neutron Resonance Transmission Imaging is an innovative and promising technique for determining both the elemental composition and the distribution of the elements inside the bulk of archaeological objects, without the need for sampling, accessing in a complementary way the region below 25 μs (that is, the epithermal range between 4.6 keV and 30 keV approximately, where intense resonances occur for several nuclides). The recent research conducted at the INES beamline of ISIS brought a dedicated measurement setup for NRTI analysis using the nGEM detector, which enables measurements with better spatial resolution than previously performed.

The application of NRTI to crucible fragments related to brass production in the ancient Roman city of Mediolanum confirms the presence of brass inclusions inside the volumes and succeeds in visualising their distribution even for those samples with no superficial depositions that could be investigated by more conventional methods, such as PIXE. Furthermore, NRTI (and NRCA) provided complementary results to the quantitative composition obtained through PIXE as arsenic, tin, antimony and silver can be detected even in very small concentrations with neutron resonant absorption reactions. The detection of these elements can be useful for characterising the alloy production process.

The NRCA investigation on the crucible fragments qualitatively confirms the overall elemental identification accomplished through NRTI.

Moreover, this kind of samples presents an inhomogeneous distribution of Cu, Sn, Sb, Ag and As. Therefore, the feasibility of the NRTI for localising the position of elements with enhanced contrast has been demonstrated through this case study. It was also possible to provide a first attempt at quantifying the detected elements, as a result of the identification of a data normalisation procedure adapted to the experimental set-up of INES and which is currently still being improved. More in-depth details on the normalisation and quantification procedure will follow in a future publication.

To conclude, the achieved results demonstrate the usefulness of NRTI to perform non-destructive imaging combined with elemental analyses for investigating the composition of inhomogeneous samples. Future steps will involve improving the NRTI spatial resolution to be competitive with other neutron imaging techniques under this feature and the quantitative calibration. Making NRTI a quantitative imaging technique can be a significant improvement in the field of neutron imaging methods. The access to bulk elemental distribution with the potential to quantify the composition with a single technique can be a significant advantage for non-destructive investigations of inhomogeneous objects that cannot be sampled (like those related to Cultural Heritage), providing complementary details to more conventional (and superficial) analytical methods.

Acknowledgements This work was partially supported by the CNR-STFC Agreement (No. 2014–2020 and No. 2020-2027), concerning collaboration in scientific research between the ISIS Neutron and Muon Source of STFC (UK) and CNR (Italy). Financial support by the Access to Research Infrastructures activity in the Horizon 2020 Programme of the EU (IPERION HS H2020-INFRAIA-01-2018-19 G.A. n. 871034) is gratefully acknowledged (FIXLAB: newAGLAE, France).

Author contributions G. M. and M.P. R. designed the research project to evaluate the feasibility of the NRTI technique for characterising the elemental composition and distribution of the crucible samples. A. S. and G. M. performed neutron experiments and data analysis. Q. L. and G. M. carried out PIXE measurements and data analysis. All authors gave contributions to the discussion of the result. G. M. wrote the manuscript in consultation with all authors. All authors have read and approved the published version of the manuscript.

Funding Open access funding provided by Università degli Studi di Milano - Bicocca within the CRUI-CARE Agreement. H2020 Excellent Science, IPERION HS H2020-INFRAIA-01-2018-19 G.A. n. 871034, Giulia Marcucci.

Data Availability Statement This manuscript has associated data in a data repository.

Declarations

Conflicts of interest There are no conflicts to declare.

References

1. I.S. Anderson, R.L. McGreevy, H.Z. Bilheux, *Neutron Imaging and Applications A Reference for the Imaging Community* (Springer, New York, 2009). (**ISBN 978-0-387-78692-6**)
2. M. Strobl et al., J. Phys. D Appl. Phys. (2009). https://doi.org/10.1088/0022-3727/42/24/243001
3. N. Kardjilov et al., Mater. Today **14**(6), 248–256 (2011). https://doi.org/10.1016/S1369-7021(11)70139-0
4. F. Salvemini et al., Neutron News **27**(2), 14–19 (2016). https://doi.org/10.1080/10448632.2016.1163982
5. N. Kardjilov et al., Mater. Today **21**(6), 652–672 (2018). https://doi.org/10.1016/j.mattod.2018.03.001
6. B. Schillinger et al., J. Imaging **4**(1), 22 (2018). https://doi.org/10.3390/jimaging4010022
7. D. Micieli et al., Sci. Rep. (2018). https://doi.org/10.1038/s41598-018-30545-z
8. N. Gelli et al., Nucl. Inst. Methods Phys. Res. Sect. A Accel. Spectrom. Detect. Assoc. Equip. **1051**, 168189 (2023). https://doi.org/10.1016/j.nima.2023.168189
9. A. Fedrigo et al., J. Phys. Conf. Ser. **2605**, 012019 (2023). https://doi.org/10.1088/1742-6596/2605/1/012019
10. S.W. Wilkins et al., Nature **384**(6607), 335–338 (1996). https://doi.org/10.1038/384335a0
11. M. Stampanoni et al., Dev. X-Ray Tomogr. V **6318**, 63180F (2006). https://doi.org/10.1117/12.679497
12. M.P. Morigi et al., Appl. Phys. A **100**, 653–661 (2010). https://doi.org/10.1007/s00339-010-5648-6
13. M.P. Morigi et al., J. Instrum. **8**(08), C08010 (2013)
14. D. Mannes et al., Phys. Procedia **69**, 653–660 (2015). https://doi.org/10.1016/j.phpro.2015.07.092
15. F. Albertin et al., Heritage **2**(3), 2028–2038 (2019). https://doi.org/10.3390/heritage2030122
16. P.J. Withers et al., Nat. Rev. Methods Primers **1**, 18 (2021). https://doi.org/10.1038/s43586-021-00015-4
17. E. Perelli Cippo et al., J. Anal. At. Spectrom. **26**(5), 992 (2011). https://doi.org/10.1039/c0ja00256a
18. G. Festa et al., J. Anal. At. Spectrom. **30**(3), 745–750 (2015). https://doi.org/10.1039/c4ja00384e
19. A. Fedrigo et al., J. Anal. At. Spectrom. **34**(12), 2420–2427 (2019). https://doi.org/10.1039/c9ja00300b
20. L. Bartoli et al., Metall. Italiana **9**, 33–39 (2008)
21. A. Pietropaolo et al., Appl. Spectrosc. **64**(9), 1068–1071 (2010). https://doi.org/10.1366/000370210792434440
22. https://www.isis.stfc.ac.uk. Accessed 16th November 2023
23. A. Ceresa Mori, C. Cucini, in Acta mineraria et Metallurgica. Studi in onore di Marco Tizzoni, Notizie Archeologiche Bergomensi, 20, (Comune di Bergamo, 2012)
24. M. Tizzoni, Notizie Archeologiche Bergomensi **4**, 111–120 (1996)
25. J. Bayley, in 2000 Years of Zinc and Brass, ed By P.T. Craddock (London: British Museum, 1998)
26. J. Bayley, al, in Hidden Histories and Records of Antiquity. Essays on Saxon and Medieval London for John Clark, Curator Emeritus, Museum of London, ed. By J. Cotton, J. Hall, J. Keily, R. Sherris, R. Stephenson (London: LAMAS , 2014) pp. 121–28
27. M. Martinón-Torres, T. Rehren, Historical Metallurgy, 36 (2002)
28. S. Merkel, Metalla **22**(1), 21–39 (2016)
29. P. Schillebeeckx et al., J. Instrum. **7**(03), 03009 (2012)
30. J. Salomon et al., Nucl. Inst. Methods Phys. Res. Sect. B Beam Interact. Mater. Atoms **266**(10), 2273–2278 (2008). https://doi.org/10.1016/j.nimb.2008.03.076
31. J. Salomon et al., Appl. Phys. A **92**, 43–50 (2008). https://doi.org/10.1007/s00339-008-4512-4
32. L. Pichon et al., Nucl. Inst. Methods Phys. Res. Sect. B **363**, 48–54 (2015). https://doi.org/10.1016/j.nimb.2015.08.086
33. M. Radepont et al., Measurement **114**, 501–507 (2018). https://doi.org/10.1016/j.measurement.2016.07.005
34. H. Postma, P. Schillebeeckx, Neutron Resonance Capture and Transmission Analysis, Encyclopedia of Analytical Chemistry (John Wiley & Sons Ltd, 2009) pp. 1–22
35. N. Kardjilov, G. Festa, Neutron methods for archaeology and cultural heritage (Springer Cham, 2017)
36. G. Noguere et al., Nuclear Inst and Methods in Physics Research, A, 575, 476–488 (2007)
37. https://atom.kaeri.re.kr/. Accessed 16th November 2023
38. F. Sauli, The gas electron multiplier (GEM): Operating principles and applications. Nucl Inst. And Meth. Phys Res A **805**, 2–24 (2016)
39. https://www.bbtech.co.jp/en/products/ngem/
40. G. Škoro, S. Lilley, R. Bewley, Phys B Phys Condens. Matter **551**, 381–385 (2018). https://doi.org/10.1016/j.physb.2017.12.060
41. P. Schillebeeckx, H. Postma, Neutron resonance analysis methods for archaeological and cultural heritage applications. In: D'Amico, S., Venuti, V. (eds) Handbook of Cultural Heritage Analysis (Springer, Cham, 2022). https://doi.org/10.1007/978-3-030-60016-7
42. C. Cazzaniga et al., AIP Adv. **11**(7), 075005 (2021). https://doi.org/10.1063/5.0043935
43. A. Subercaze et al., Nucl. Inst. Methods Phys. Res. Sect. B **406**, 104–107 (2017). https://doi.org/10.1016/j.nimb.2017.02.014
44. P.T. Craddock, J. Archaeol. Sci. **5**(1), 1–16 (1978). https://doi.org/10.1016/0305-4403(78)90015-8
45. A. Pollard et al., Antiquity **89**(345), 697–713 (2015). https://doi.org/10.15184/aqy.2015.20